Laser-Plasma Physics at >10 PW

Andrea Macchi

National Institute of Optics, National Research Council (CNR/INO),
Adriano Gozzini research unit, Pisa, Italy

Enrico Fermi Department of Physics, University of Pisa, Italy

Central Laser Facility, RAL, Didcot (UK), December 1, 2016

Outline

- Radiation pressure acceleration (RPA): reaching relativistic speed
  - the role of laser polarization
  - fast & efficient “Light Sail” RPA
- Plasmonic-enhanced Rayleigh-Taylor instability
- Radiation friction (RF) losses in RPA: thick vs thin targets
- RF-driven Inverse Faraday Effect: generation of Gigagauss magnetic fields

Early vision of radiation pressure acceleration (1966)

22 NATURE JULY 2, 1966 VOL. 211

INTERSTELLAR VEHICLE PROPELLED BY TERRESTRIAL LASER BEAM

By PROF. G. MARX

Institute of Theoretical Physics, Roland Eötvös University, Budapest

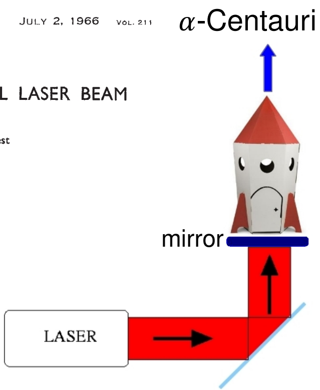

A solution to “Fermi’s paradox”: “*Laser propulsion from Earth . . . would solve the problem of acceleration but not of deceleration at arrival . . . no planet could be invaded by unexpected visitors from outer space*”

Starshot: laser-boosted light sails for space travel

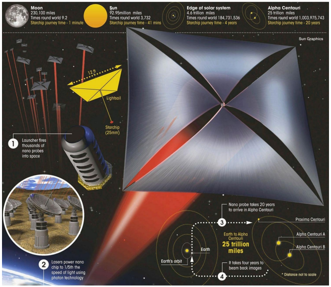

(credit: Breakthrough Starshot, breakthroughinitiatives.org)

Goal: accelerating a sail to V=0.2c
Critical analysis: H. Milchberg, "Challenges abound for propelling interstellar probes"
Physics Today, 26 April 2016

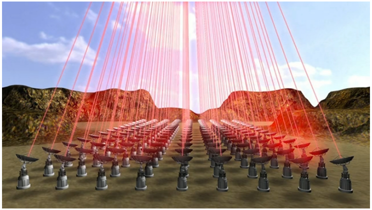

The accelerating mirror model of RPA

Perfect mirror boosted by a plane wave: momentum transfer (i.e. force) by light and mechanical efficiency η may be derived considering Doppler shifted reflection and number conservation of photons

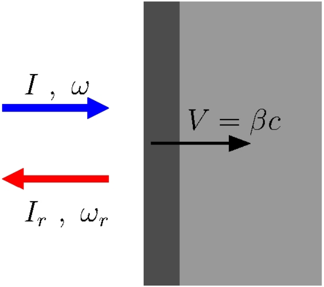

$$\frac{dp}{dt} = \frac{2I}{c}\frac{1-\beta}{1+\beta} \qquad \eta = \frac{2\beta}{1+\beta}$$

As $\beta \longrightarrow 1$: high efficiency ($\eta \to 1$) but slow gain ($dp/dt \to 0$)

RPA in thick and thin targets

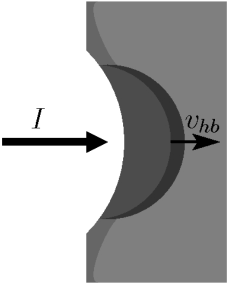

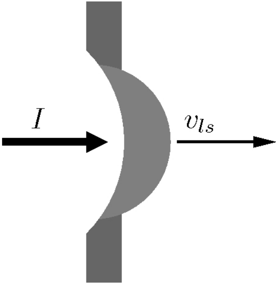

Hole Boring (HB): thick target swept by RPA as a "snwoplow"

Light Sail (LS): thin target pushed as a whole

Using ultrathin (nm) targets and high contrast PW pulses, relativistic velocities may be reached via LS acceleration!

How to make radiation pressure dominant?

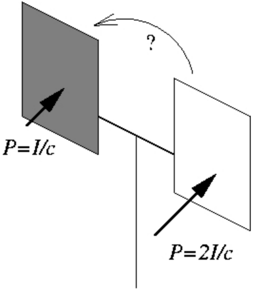

The “Optical Mill” rotates in the *opposite* sense to that suggested by radiation pressure balance: due to imperfect vacuum *thermal* pressure due to heating dominates

Enforcing radiation pressure dominance requires to minimize heating of the target

Polarization suppression of electron heating

At normal incidence on a "solid" target, electrons are heated via non-linear, non-adiabatic oscillations driven by the "$\mathbf{v} \times \mathbf{B}$" magnetic force term across the sharp laser-vacuum interface

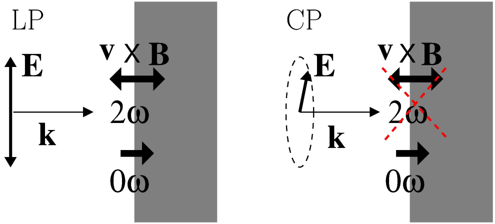

Using circular polarization (CP), the oscillating ("2ω") term in $\mathbf{v}\times\mathbf{B}$ cancels out and electron heating is strongly reduced
[Macchi et al, Phys. Rev. Lett. **95** (2005) 185003]

Light Sail formulas from plane moving mirror model

Energy per nucleon $\mathscr{E}_{\rm n}$ as a function of pulse intensity I and duration τ_p and of areal density $\rho\ell$

$$\mathscr{E}_{\rm n}^{\rm max} = m_p c^2 \frac{\mathscr{F}^2}{(2(\mathscr{F}+1))} \qquad \left(\mathscr{F} = \frac{2I\tau_p}{\rho\ell}\right)$$

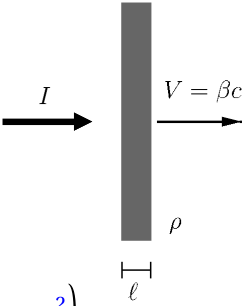

($\mathscr{E}_{\rm n}$>100 MeV using GEMINI with $\ell \simeq 10$ nm)

$$\mathscr{E}_{\rm n}(t) \propto \left(\frac{2It}{\rho\ell c^2}\right)^{1/3} \qquad \left(t \gg \frac{\rho\ell c^2}{I}\,, V \to c\,, \mathscr{E}_{\rm n} > m_p c^2\right)$$

Favorable scaling of $\mathscr{E}_{\rm n}$ with $\mathscr{F}$ (and monoenergetic spectrum expected for coherent, “rigid”, sail motion) BUT slow gain in the relativistic regime (issues of laser diffraction, foil stability, . . .)

“Unlimited” acceleration in 3D

Transverse expansion of the target reduces surface density $\rho\ell \longrightarrow$ light sail gets “lighter” $\longrightarrow$ enhanced acceleration (at the expense of the number of ions)
[S.V.Bulanov et al, PRL **104** (2010) 135003]

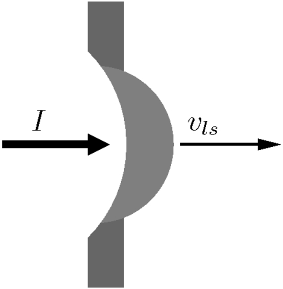

Faster gain $\mathscr{E}_{\rm n}(t) \simeq \left(\dfrac{2It}{\rho\ell c^2}\right)^{3/5}$ predicted in 3D

The mechanism is effective for *relativistic* velocity which also increases target reflectivity (the laser frequency decreases in the moving sail frame)

3D simulation of “unlimited” acceleration

Laser: 24 fs, 4.8 μm spot, $I = 0.85 \times 10^{23}$ W cm^{-2}
Target: $\ell = 1$ μm H foil, $n_e = 10^{23}$ cm^{-3} $U \simeq 1.5$ kJ , $P \simeq 60$ PW

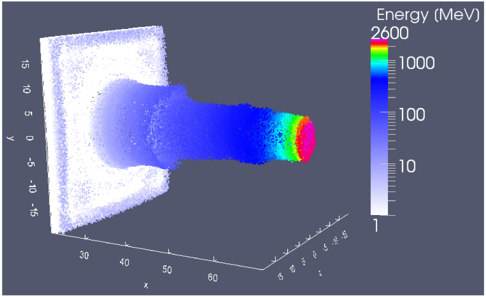

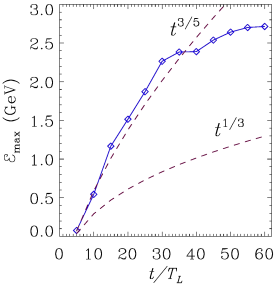

$\mathcal{E}_{\max} \simeq 2.6$ GeV > 4X 1D model prediction
Sgattoni, Sinigardi, Macchi, Appl. Phys. Lett. **105** (2014) 084105

CH foil simulation and 3D vs 2D

C+H double layer foil , $n_C = (64/6)n_c$, $n_H = 8n_c$

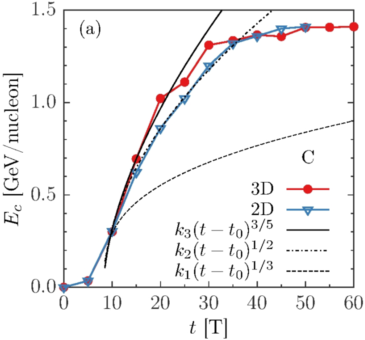

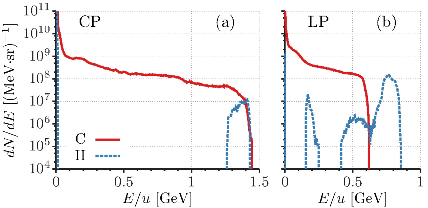

Circular vs Linear Polarization: Higher energy and narrower H (proton) spectrum for CP

Onset of transparency stops acceleration and is faster in 3D than in 2D → similar final energy in 2D and 3D (~1.4 GeV for CP)

Sgattoni et al, APL **105** (2014) 084105

Foil breakup: structures in ion density

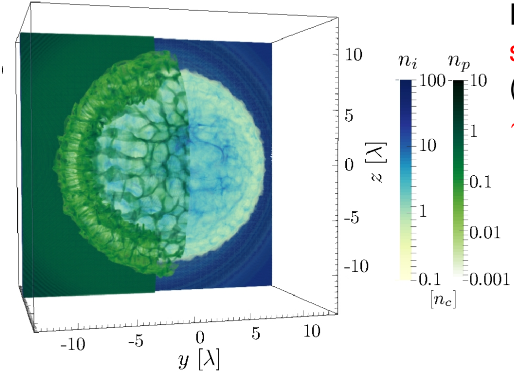

Two species target - protons and carbon ions

Formation of net-like structures with size $\sim \lambda$ (laser wavelength) and $\sim$ hexagonal shape

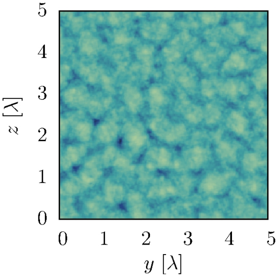

A. Sgattoni, S. Sinigardi, L. Fedeli, F. Pegoraro, A. Macchi, Phys. Rev. E **91** (2015) 013106

Rayleigh-Taylor Instability in space and lab plasmas

Crab Nebula, Hubble Space Telescope

Laser-driven implosion for Inertial Confinement Fusion studies, 1995 (Wikipedia)

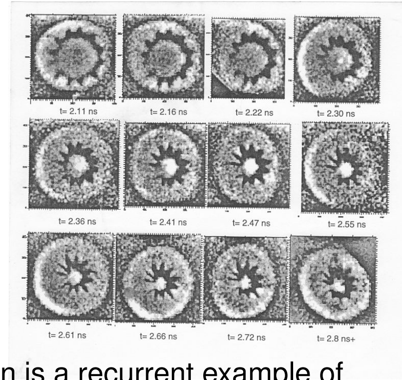

Hexagon formation is a recurrent example of spontaneous symmetry breaking in 3D RTI

S.I.Abarzhi, Phys. Rev. E **59** (1999) 1729; D.Schattschneider, Amer. Math. Monthly **85** (1978) 439

Rayleigh-Taylor Instability in RPA-LS

A thin foil of areal density $\rho\ell$ accelerated by a pressure $P = 2I/c$ is unstable: growth of transverse ripples with wavevector q at a rate $\gamma = (Pq/\rho\ell)^{1/2}$ [E. Ott, PRL **29** (1972) 1429]

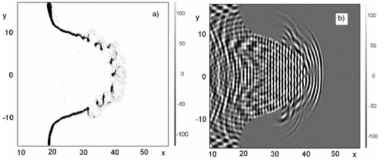

2D simulation
[F.Pegoraro & S.V.Bulanov, PRL **99** (2007) 065002]

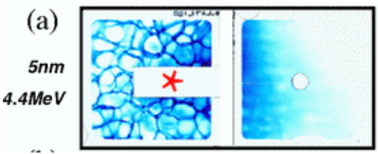

Experimental indication from accelerated ion beam profile structures [C.Palmer et al, PRL **108** (2012) 225002]

What sets the dominant wavevector $q \sim (2\pi/\lambda)$?

Plasmonic-enhanced modulation of radiation pressure

The EM field at a 2D sinusoidally rippled surface (grating) of period d) is modulated with resonant plasmonic enhancement of the P-component when $d \sim \lambda$

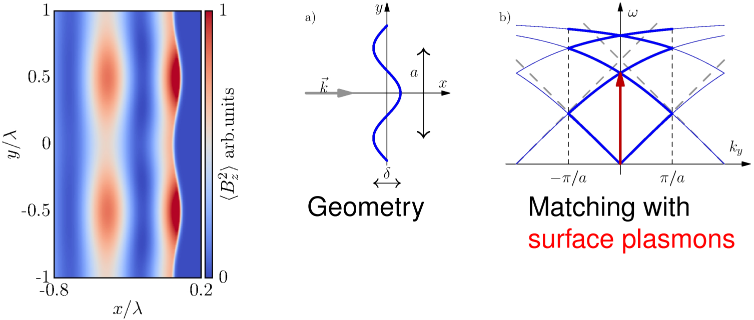

Geometry

Matching with surface plasmons

Theory: A. Sgattoni et al, Phys. Rev. E **91** (2015) 013106;
B. Eliasson, New J. Phys. **17** (2015) 033026

Radiation friction effects on RPA

- At irradiances $I\lambda^2 > 10^{23}$ W cm$^{-2}\mu$m^2 the energy loss by incoherent radiation emission (as X- and γ-rays) may become relevant
- In a classical framework, radiative losses may be included by inserting the radiation friction (RF) force (aka radiation reaction)

$$\frac{d\mathbf{p}}{dt} = -e\left(\mathbf{E} + \frac{\mathbf{v}}{c} \times \mathbf{B}\right) + \mathbf{f}_{\rm rad}$$

- Landau-Lifshitz expression for $\mathbf{f}_{\rm rad}$

$$\begin{aligned} \mathbf{f}_{\rm rad} \quad = \quad & -\frac{2r_c^2}{3}\left\{\gamma^2\left[\left(\mathbf{E} + \frac{\mathbf{v}}{c} \times \mathbf{B}\right)^2 - \left(\frac{\mathbf{v}}{c}\cdot\mathbf{E}\right)^2\right]\frac{\mathbf{v}}{c}\right. \\ & \left. -\left[\left(\mathbf{E} + \frac{\mathbf{v}}{c} \times \mathbf{B}\right)\times\mathbf{B} + \left(\frac{\mathbf{v}}{c}\cdot\mathbf{E}\right)\mathbf{E}\right] + \gamma\frac{m_e c}{e}\left(\frac{d\mathbf{E}}{dt} + \frac{\mathbf{v}}{c} \times \frac{d\mathbf{B}}{dt}\right)\right\} \end{aligned}$$

Light Sail 3D simulation: CP, no RF

Ions

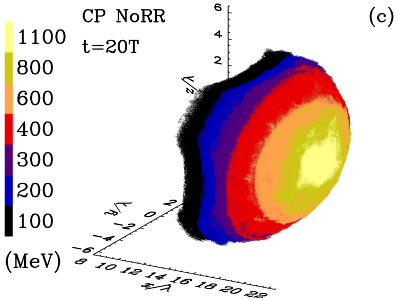

Electrons

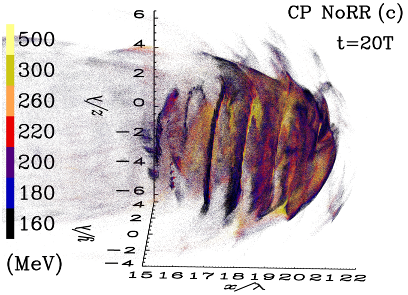

Symmetric, collimated space-energy distribution of ions

"Screw-like" electron distribution with a tail

[Tamburini, Liseikina, Pegoraro, Macchi, Phys.Rev.E **85** (2012) 016407]

Light Sail 3D simulation: CP, with RF

Ions

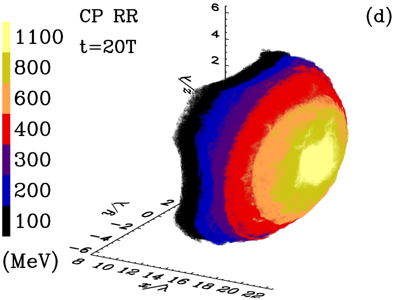

Electrons

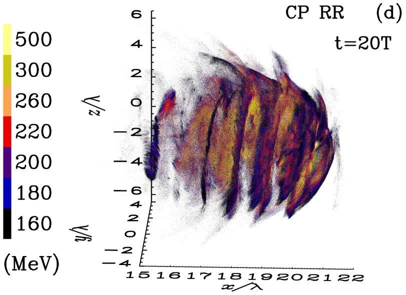

Ion distribution unchanged by RF

Cooling of electrons in pulse tail due to radiative losses

[Tamburini, Liseikina, Pegoraro, Macchi, Phys.Rev.E **85** (2012) 016407]

Light Sail 3D simulation: LP, no RF

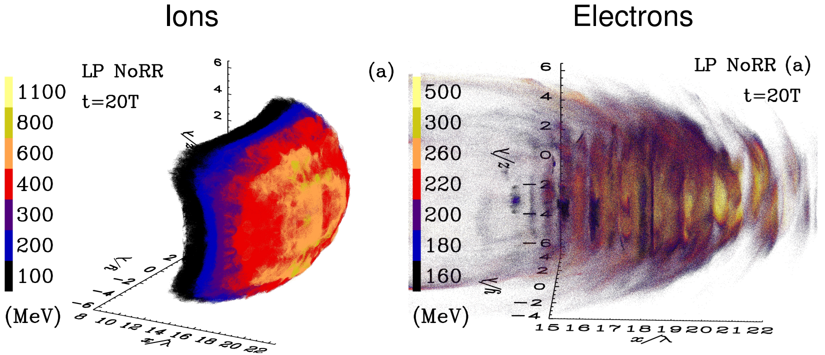

Asymmetric distribution with highest energy ions off-axis

Cut-off energy of ~ 0.9 GeV much lower than for CP

[Tamburini, Liseikina, Pegoraro, Macchi, Phys.Rev.E **85** (2012) 016407]

Light Sail 3D simulation: LP, with RF

Ions

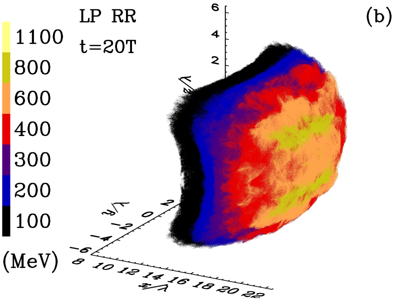

Electrons

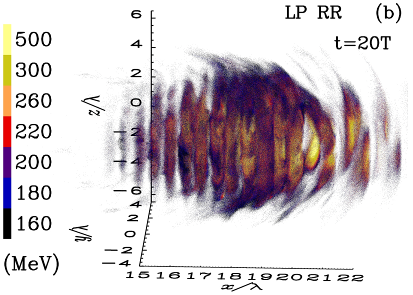

Strong cooling of electrons reduces pulse transmission

Cut-off energy is *increased* up to ~ 1.1 GeV by RF

[Tamburini, Liseikina, Pegoraro, Macchi, Phys.Rev.E **85** (2012) 016407]

Polarization effect on RF losses

Radiation power for an electron in a plane wave with

$\mathbf{k} = (\omega/c)\hat{\mathbf{x}}$, $\mathbf{v} = v_x\hat{\mathbf{x}}$ $\quad \left(a_0 \equiv \frac{eE}{m_e\omega c}\right)$

$$P_{\text{rad}} = \mathbf{f}_{\text{rad}} \cdot \mathbf{v} \simeq \frac{2e^2\omega^2\gamma^2 a_0^2}{3c}\left(1 - \frac{v_x}{c}\right)^2$$

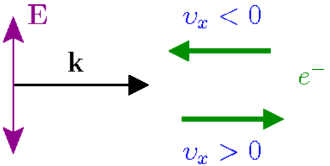

For CP, electrons move coherently with the foil at $v_x \sim c \longrightarrow \mathbf{f}_{\text{rad}} \simeq 0$

For LP, the *oscillating* term in the $\mathbf{v} \times \mathbf{B}$ force causes $v_x \sim -c$ periodically

$\longrightarrow$ "colliding" geometry maximizes $\mathbf{f}_{\text{rad}}$

$\longrightarrow$ significant radiative losses

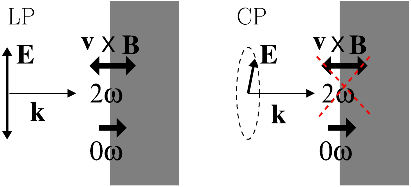

RF losses in thick targets

- RF losses are small for thin targets pushed by CP pulses
- BUT simulations show major RF losses (up to $\sim 40\%$ already at $I = 4 \times 10^{22}$ W cm^{-2}) for thick targets also for CP [Naumova et al, PRL **102** (2009) 25002; Schlegel et al, PoP **16** (2009) 83103; Capdessus et al., PRE **86** (2012) 036401; Nerush & Kostyukov, PPCF **57** (2015) 35007]
- Our model:
  oscillations of the "hole boring" front
  during "snowplow" acceleration produce
  bunches of "returning",
  counterpropagating electrons
  $\rightarrow$ collective "collisions" with the laser pulse
  $\rightarrow$ high RF losses

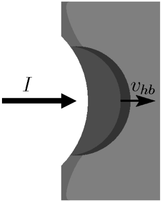

Beyond the mirror: hole boring dynamics

Real targets are not "perfect rigid mirrors":

- the ponderomotive force (PF) i.e. the "local" radiation pressure separates electrons from ions
- the charge-separation field E_x balances the PF
- E_x accelerates ions, bunching them in the "skin" layer
- a density spike is generated and "wavebreaking" occurs:

HB is a pulsed process [Macchi et al, PRL **94** (2005) 165003]

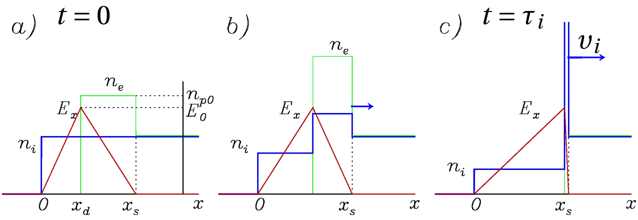

Model for returning electrons in thick targets

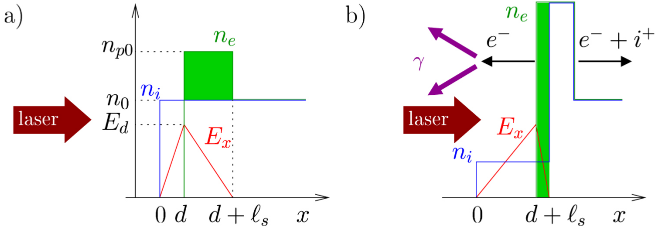

- The PF generates an excess of electrons in the skin layer ($d < x < d + \ell_s$) and of ions in the depletion layer ($0 < x < d$)
- At the end of the acceleration stage ($t = \tau_i$) i.e. at wavebreaking equilibrium between electrostatic and ponderomotive forces is lost

→ the excess electrons return towards the laser in a time τ_e and radiate efficiently

Estimating the number of returning electrons

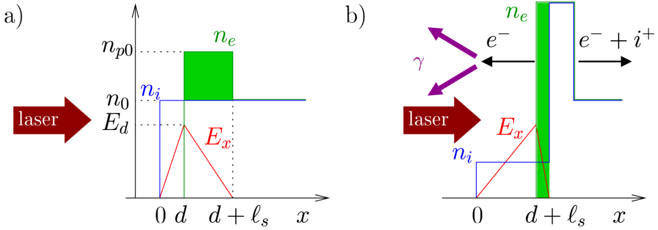

- $eE_0 n_{p0}\ell_s/2 \simeq 2I/c$ (pressure balance)
- $E_0 = 4\pi e n_0 d$ (Poisson-Gauss equation)
- $n_{p0}\ell_s = n_0(d+\ell_s)$ (charge conservation)

→ $N_x = (n_{p0} - n_0)\ell_s \simeq n_{p0}\ell_s \simeq a_0/r_c\lambda$
returning electrons per unit surface ($r_c = e^2/m_e c^2$)

Estimating radiation from returning electrons

- Fraction of laser energy re-emitted as radiation from N_x electrons with $(1 - v_x/c) \gtrsim 1$ (thus $P_{\text{rad}} \simeq 2e^2\omega^2\gamma^2 a_0^2/3c$)

$$\eta_{\text{rad}} \equiv \frac{P_{\text{rad}} N_x}{I_L} \frac{\tau_e}{\tau_e + \tau_i} \approx \frac{4\pi}{3} \frac{r_c}{\lambda} \gamma^2 a_0 \qquad (\text{if } \tau_e \approx \tau_i)$$

- If $\gamma = (1 + a_0^2)^{1/2} \simeq a_0$ $\qquad (a_0 \gg 1, |p_x| \ll |p_\perp|)$

$$\eta_{\text{rad}} \simeq \frac{4\pi}{3} \frac{r_c}{\lambda} a_0^3 \sim 1 \text{ for } a_0 = 400 \; (\lambda = 0.8\mu\text{m})$$

i.e. at $I \simeq 7 \times 10^{23}$ W cm^{-2} radiative losses would exceed the laser energy!

Angular momentum absorption

- A CP laser pulse carries "spin" angular momentum (AM) that may be absorbed by the target

$$L_z = \int_0^\infty \ell_z(r) 2\pi r \mathrm{d}r = -\int_0^\infty \frac{r}{2c\omega} \partial_r I(r) 2\pi r \mathrm{d}r$$

- Reflection from a perfect mirror conserves number of photons and does *not* change sign of "spin"

$\rightarrow$ No AM absorption without "dissipation"

- Can RF provide efficient dissipation for AMA?
- Does RF-induced AMA leads to generation of an axial magnetic field ("Inverse Faraday Effect", IFE)?

Searching for IFE in 3D thick target simulations

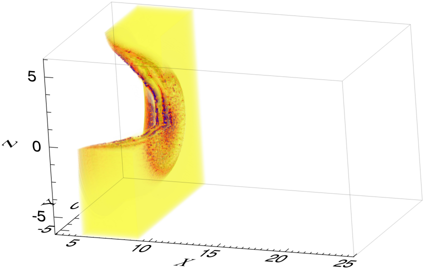

$\lambda = 0.8\ \mu$m
$n_e = 90 n_c = 1.6 \times 10^{23}$ cm^{-3}
$a_0 = (200 - 600)$
$I = (0.9 - 7.8) \times 10^{23}$ W cm^{-2}
$U = (0.4 - 4) \times 10^3$ J

Laser pulse at waist (target boundary)

$$\mathbf{a}(x=0,r,t) = a_0 \left(\hat{\mathbf{y}} \cos(\omega t) \pm \hat{\mathbf{z}} \sin(\omega t)\right) \mathrm{e}^{-(r/r_0)^n - (ct/r_l)^4}$$

$n = 2$ (Gaussian profile) or $n = 4$ (super-Gaussian)
$r_l = 3\lambda$, $r_0 = 3.8\lambda$

Gigagauss axial magnetic fields induced by RF -I

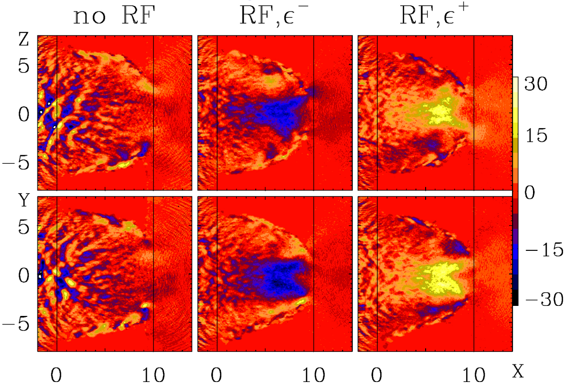

B_x

units:
$B_0 = m_e c\omega/e$
$= 1.34 \times 10^8$ G

No axial field without RF
Sign of B_x changes with laser pulse helicity

T. V. Liseykina, S. V. Propruzhenko, A. Macchi, New J. Phys. **18** (2016) 072001

Gigagauss axial magnetic fields induced by RF -II

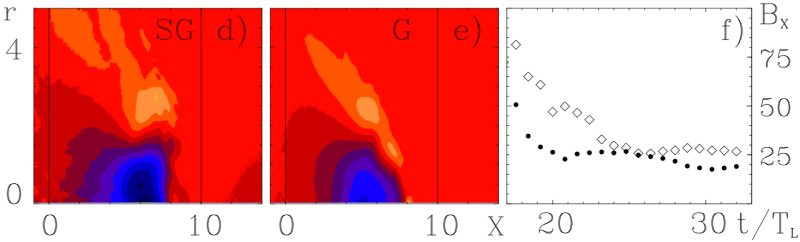

Similar results for Gaussian and Super-Gaussian profiles

The axial **B**-field is quasi-steady after the laser pulse

Peak amplitude $B_{\max} \simeq 28 B_0 \simeq 5 \times 10^9$ G for $a_0 = 500$

T. V. Liseykina, S. V. Propruzhenko, A. Macchi, New J. Phys. **18** (2016) 072001

Unexpected (and embarassing) hype . . .

physicsworld.com

Home | News | Blog | Multimedia | In depth | Events

News archive

- 2016
  - October 2016
  - September 2016
  - August 2016
  - July 2016
  - June 2016
  - May 2016
  - April 2016
  - March 2016
  - February 2016
  - January 2016
- 2015
- 2014
- 2013
- 2012
- 2011
- 2010
- 2009
- 2008
- 2007
- 2006
- 2005
- 2004

'Radiation friction' could make huge magnetic fields with lasers

Jul 19, 2016 2 comments

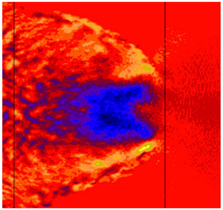

Facts On File **Today's Science**
Science News Written Especially for Students

FILED UNDER: ASTROPHYSICS | ELECTROMAGNETISM | ELECTRONICS AND ELECTROMAGNETISM | MOTIONS AND FORCES | OPTICS | PARTICLES | PRO | RESEARCH METHODS (PHYSICS)

How to Create the World's Strongest Magnet

PHYS.ORG Nanotechnology Physics Earth Astronomy & Space Technology Chemistry Biology

search

Home » Physics » General Physics » August 10, 2016

New method for generating superstrong magnetic fields

August 10, 2016

Science alert

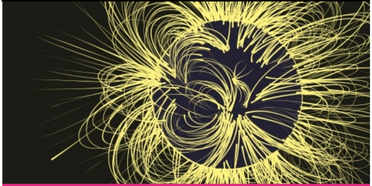

Physicists have calculated a whole new way to generate super-strong magnetic fields

Stronger than any magnetic field on Earth.

Gigagauss fields as a test bed for RF?

- Radiation friction is a longstanding, open problem both in classical and quantum electrodynamics, but experiments have not tested different models yet
- Most experimental proposals are based on single particle effects, which require high precision measurements
- RF-induced IFE is a robust, unambigous, collective signature of RF effects which might be used as a test bed of different theories
- MG fields generated by IFE due to collisional friction at “low” intensities (10^{19} W cm^{-2}) were observed via ultrafast detection of polarization rotation of a probe pulse (“direct” Faraday effect) on VULCAN

  Z. Najmudin et al, Phys. Rev. Lett. **87** (2001) 215004

Scaling with a_0 and angular momentum absorption

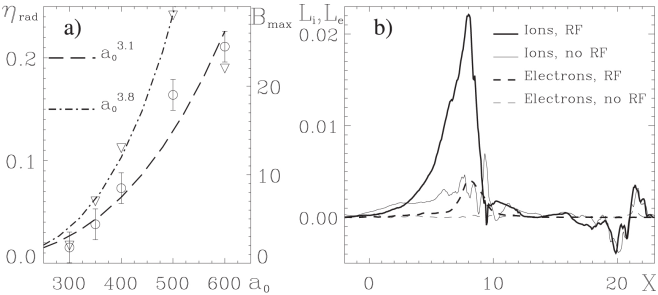

Scaling with a_0:
Radiative loss $\eta_{\rm rad} \sim a_0^3$
(max value $\sim 25\%$)
Peak field $B_{\rm max} \sim a_0^4$

Mechanical AM
$L_{e/i}(x) = \int n_{e/i}(\mathbf{r} \times \mathbf{p})dydz$
$L_i \gg L_e$: most of AM eventually goes to ions

Analytical model of IFE

- Model inspired by IFE theory developed for the VULCAN experiment
  M. G. Haines, Phys. Rev. Lett. **83** (2001) 165003
  "*[This] theory of axial magnetic field generation [. . .] contrasts markedly with existing theories of the inverse Faraday effect*"
- Our analytical predictions:

$$\frac{B_{xm}}{B_0} \simeq \frac{0.2}{\pi}\eta_{\text{rad}}\frac{r_l\lambda}{R\delta}a_0 \propto a_0^4 \qquad \frac{L_i}{L_e} \simeq \frac{Am_p}{Zm_e} \gg 1$$

(r_l, R: pulse length and radius, δ: thickness of the AM deposition layer)
in qualitative agreement with simulation •
T. V. Liseykina, S. V. Propruzhenko, A. Macchi,
New J. Phys. **18** (2016) 072001

Coworkers

A. Sgattoni[1,⋆], L. Fedeli[2,1,†], S. Sinigardi[1,‡], F. Pegoraro[2,1], T. V. Liseykina[3,∘], S. V. Propruzhenko[4]

[1] *CNR/INO, Pisa, Italy*
[2] *Dipartimento di Fisica Enrico Fermi, Università di Pisa, Italy*
[3] *Institute of Physics, University of Rostock, Germany*
[4] *National Research Nuclear University, Moscow Engineering Physics Institute, Russia*

[⋆] *presently at LULI-UPMC, Paris, and LESIA, Observatoire de Paris, France*
[†] *presently at Dipartimento di Energia, Politecnico di Milano, Italy*
[‡] *presently at Dipartimento di Fisica e Astronomia & INFN, Università di Bologna, Italy*
[∘] *on leave from Institute of Computational Technologies, SD RAS, Novosibirsk, Russia*

EXTRA SLIDES

Thin foil RTI with self-consistent pressure modulation

Model: reflection from shallow 2D grating of depth δ (first order in δ/λ) + modified Ott's theory[1] with modulated pressure:

$$P \simeq P_0\left(1 + K(q)\delta\cos qy\right)\,, \qquad K(q) = \begin{cases} -(q^2-k^2)^{1/2} & (S) \\ k^2(q^2-k^2)^{-1/2} & (P) \\ (k^2-q^2/2)(q^2-k^2)^{-1/2} & (C) \end{cases}$$

$$\gamma = (P_0/\sigma)^{1/2}\left[\left(q^2 + K^2(q)/4\right)^{1/2} + K(q)/2\right]^{1/2}$$

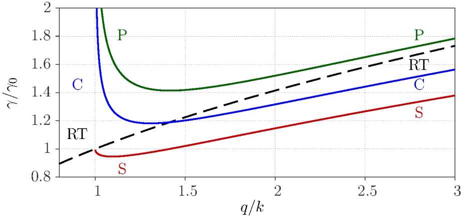

S-polarization
P-polarization
C-ircular polarization
RT: no modulation ($\delta = 0$)

[1] E. Ott, PRL **29** (1972) 1429

Symmetry of RTI structures

Hexagonal-like structures generated by nonlinear evolution of RTI: an example of spontaneous symmetry breaking in a classical system with “wallpaper” p6m symmetry

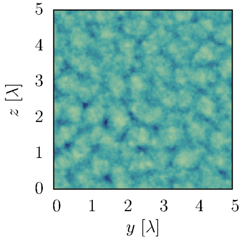

S.I.Abarzhi, PRE **59** (1999) 1729
D.Schattschneider, Amer. Math. Monthly **85** (1978) 439

A. Sgattoni, S. Sinigardi, L. Fedeli, F. Pegoraro, A. Macchi, PRE **91** (2015) 013106

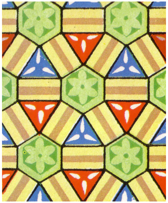

Persian glazed tile

Relativistic Landau-Lifshitz RF force

Aim: making electron dynamics consistent with radiation emission (i.e. self-generated fields)

$$\begin{aligned}
\frac{dp^\mu}{d\tau} &= -eF^{\mu\nu}u_\nu + f^\mu_{\text{rad}} \\
f^\mu_{\text{rad}} &= -\frac{2r_c^2}{3}\left[F^{\mu\nu}F_{\alpha\nu}u^\alpha - F^{\alpha\nu}u_\nu F_{\alpha\beta}u^\beta u^\mu + \frac{m_e c}{e}\partial_\alpha F^{\mu\nu}u^\alpha u_\nu\right]
\end{aligned}$$

Spatial component in the laboratory frame:

$$\begin{aligned}
\mathbf{f}_{\text{rad}} &= -\frac{2r_c^2}{3}\left\{\gamma^2\left[\left(\mathbf{E}+\frac{\mathbf{v}}{c}\times\mathbf{B}\right)^2 - \left(\frac{\mathbf{v}}{c}\cdot\mathbf{E}\right)^2\right]\frac{\mathbf{v}}{c}\right. \\
&\quad \left. -\left[\left(\mathbf{E}+\frac{\mathbf{v}}{c}\times\mathbf{B}\right)\times\mathbf{B} + \left(\frac{\mathbf{v}}{c}\cdot\mathbf{E}\right)\mathbf{E}\right] + \gamma\frac{m_e c}{e}\left(\frac{\mathrm{d}\mathbf{E}}{\mathrm{d}t} + \frac{\mathbf{v}}{c}\times\frac{\mathrm{d}\mathbf{B}}{\mathrm{d}t}\right)\right\}
\end{aligned}$$

“Reduced” LL model

[M. Tamburini, F. Pegoraro, A. Di Piazza, C. H. Keitel, A. Macchi, New J. Phys. **10**, 123005 (2010)]

$$\mathbf{f}_{\text{rad}} = -\left(\frac{2r_c^2}{3}\right) \times \left\{ \gamma^2 \left[\left(\mathbf{E} + \frac{\mathbf{v}}{c} \times \mathbf{B}\right)^2 - \left(\frac{\mathbf{v}}{c} \cdot \mathbf{E}\right)^2 \right] \frac{\mathbf{v}}{c} - \left[\left(\mathbf{E} + \frac{\mathbf{v}}{c} \times \mathbf{B}\right) \times \mathbf{B} + \left(\frac{\mathbf{v}}{c} \cdot \mathbf{E}\right) \mathbf{E} \right] \right\}$$

- Spin force and smaller term containing $\partial_t \mathbf{E}$, $\partial_t \mathbf{B}$ are neglected in $\mathbf{f}_{\text{rad}}$
- Chosen by other groups, e.g. OSIRIS team after extensive comparison [Vranic et al, Comp. Phys. **204** (2016) 141]

Kinetic equation with RF included

Equation for distribution function $f_e = f_e(\mathbf{r}, \mathbf{p}, t)$

$$\partial_t f_e + \nabla_{\mathbf{r}} \cdot (\mathbf{v} f_e) + \nabla_{\mathbf{p}} \cdot (\mathbf{f} f_e) = 0 \qquad (1)$$

$$\mathbf{f} = -e(\mathbf{E} + \mathbf{v} \times \mathbf{B}/c) + \mathbf{f}_{\text{rad}}, \qquad \nabla_{\mathbf{p}} \cdot (\mathbf{f}_{\text{rad}} f_e) = 0 \neq \mathbf{f}_{\text{rad}} \cdot \nabla_{\mathbf{p}} f_e$$

$\longleftarrow$ the PIC approach provides a solution of (1)

Entropy decrease and phase space contraction because of RF cooling effect

$$\frac{\mathrm{d}}{\mathrm{d}t} \int f_e \ln f_e \mathrm{d}^3\mathbf{p}\mathrm{d}^3\mathbf{q} = \int f_e \nabla_{\mathbf{p}} \cdot (\mathbf{f}_{\text{rad}}) \mathrm{d}^3\mathbf{p}\mathrm{d}^3\mathbf{q} < 0$$

[M. Tamburini et al, NIMA **653** (2011) 181]

Analytical theory of IFE - 1

Angular momentum density peaks at the beam edge ($r = R \simeq r_0$)

$$\mathscr{L}_x = (\mathbf{r} \times (\mathbf{E} \times \mathbf{B}))_x / 4\pi c = -r\partial_r I_L(r)/(2c\omega)$$

$\longrightarrow$ ion and electron fluids modeled as thin rigid cylinders with momenta of inertia $\mathscr{I}_e = 2\pi R^3 \delta h m_e n_e$, $\mathscr{I}_i = (Am_p/Zm_e)\mathscr{I}_e$

Torque by AMA on electrons $M_{\text{abs}} \simeq P_{\text{abs}}/\omega \simeq P_{\text{rad}}/\omega$

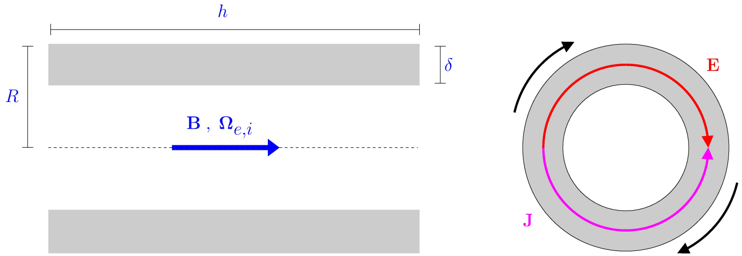

Analytical theory of IFE - 2

Induced $\mathbf{E}$-field exerts opposite torques on ions and electrons

$$\frac{dL_e}{dt} = \mathscr{I}_e \frac{d\Omega_e}{dt} = M_{\text{abs}} - M_E \qquad \frac{dL_i}{dt} = \mathscr{I}_i \frac{d\Omega_i}{dt} = M_E$$

$$E_\phi = -(r/2c)\partial_t B_x \qquad M_E = \int n_e e E_\phi r \mathrm{d}^3 r \simeq \frac{eE_\phi(R)}{m_e R}\mathscr{I}_e$$

Electron current density $j_{e\phi} \simeq -en_e\Omega_e R$

"Solenoid" approximation $B_x \simeq 4\pi j_{e\phi}\delta/c$

$$\longrightarrow M_E \simeq \frac{\omega_p^2 R\delta}{2c^2}\mathscr{I}_e \frac{d\Omega_e}{dt} \equiv \mathscr{I}'_e \frac{d\Omega_e}{dt}$$

$\longrightarrow$ Induction effects are equivalent to additional inertia

Analytical theory of IFE - 3

$$\Omega_e(t) = \frac{1}{\mathcal{I}_e + \mathcal{I}_e'} \int_0^t M_{\text{abs}}(t')dt'$$

"Induction inertia" dominates for electrons

$$\mathcal{I}_e' \sim (\omega_p^2/\omega^2)\mathcal{I}_e = (n_e/n_c)\mathcal{I}_e \gg \mathcal{I}_e$$

$$\longrightarrow M_{\text{abs}} - M_E = \mathcal{I}_e \frac{d\Omega_e}{dt} \simeq 0$$

$$\longrightarrow L_i \simeq \int_0^t M_{\text{abs}}(t')dt' \simeq \frac{\mathcal{I}_e'}{\mathcal{I}_e} L_e \gg L_e$$

in agreement with simulations

Analytical theory of IFE - 4

Posing $M_{\text{abs}} \simeq M_E$ allows to obtain E_ϕ and $\partial_t B_x$ from M_{abs}
Peak magnetic field $B_{xm} = B_x(r = 0, t = \infty)$

$$\frac{\pi e}{c} n_e h R^3 \delta B_{xm} \simeq \int_0^\infty M_{\text{abs}}(t)\,dt \simeq \frac{U_{\text{abs}}}{\omega} = \eta_{\text{rad}} \frac{U_{\text{L}}}{\omega}$$

$n_e h \simeq 2 n_c a_0 c/\omega$ from HB model

$$\frac{B_{xm}}{B_0} \simeq \frac{0.2}{\pi} \eta_{\text{rad}} \frac{r_l \lambda}{R\delta} a_0 \quad \propto a_0^4$$

scaling in agreement with simulations •

Analytical theory of IFE - 5

Estimate of B_{xm} from empirical value $\eta_{\text{rad}} \simeq 0.24$ and using "vacuum" laser parameters $R \simeq r_0 = 3.8\lambda$ and $\delta \simeq \lambda$

$$B_{xm} \simeq 4.8 B_0$$

Considering dynamical evolution of the pulse (self-channeling and focusing, radial profile steepening) yielding $R \simeq 2\lambda$, $\delta \simeq 0.5\lambda$ and $a(r = 0) \simeq 1.2 a_0$

$$B_{xm} \simeq 23 B_0$$

fair agreement with numerical observation